Available online at www.sciencedirect.com

SciVerse ScienceDirect

Procedia Engineering 58 (2013) 363 – 368

Procedia Engineering

www.elsevier.com/locate/procedia

The 12th Hypervelocity Impact Symposium

Imaging Ejecta and Debris Cloud Behavior Using Laser Side-Lighting

J.M. Mihaly[a]*, A.J. Rosakis[a], M.A. Adams[a], J.T. Tandy[a]

[a]*Graduate Aerospace Laboratories, California Institute of Technology, Pasadena, CA, United States*

Abstract

The Caltech Small Particle Hypervelocity Impact Range (SPHIR Facility) utilizes a two-stage, light gas gun to accelerate Nylon 6/6 right cylinders (d = 1.8 mm, L/D=1, 5.5 mg) and spheres (d = 1.8 mm, 3.6 mg) to impact speeds of 5 km/s and above. The projectiles impact aluminum 6061-T6 plate targets. An optical technique was employed to produce images of the hypervelocity impact event with short exposure times (20 ns) and short inter-frame times (<1 μs). The technique uses coherent illumination, orthogonal to the projectile flight direction, to provide a series of shadowgraph images of the impact on the target. An expanded beam from a 532 nm continuous wave laser is used as the illumination source. The beam is expanded to illuminate a 10 cm diameter area and is then directed to a gated, intensified high-speed CCD camera. The front ejecta and debris clouds created behind the target are simultaneously imaged with this system. An edge-finding algorithm has been developed to provide a consistent method for identifying the position of the debris-front in sequential images. This technique enables a regular method to investigate the debris cloud evolution and to characterize its asymmetrical features. Furthermore, with the Laser Side-lighting system atmospheric waves emanating from the impact site are also visible. Increasing the atmospheric pressure in the target chamber (above the nominal 1.5 Torr) significantly increases the observable features of these shock waves. The behaviour of these waves provides an improved understanding of the temporal sequence of the impact phenomena.

Keywords: High-Speed Imaging, Laser Shadowgraph, Debris Cloud, Ejecta

Nomenclature

SPHIR	Small Particle Hypervelocity Impact Range
LSL	Laser Side-Lighting
d	Impactor diameter, mm
h	Target plate thickness, mm
v	Impact speed, km/s

1. Introduction

Damage from the hypervelocity impact of meteoroids and orbital debris (MOD) poses a serious and growing threat to spacecraft. Historically, the cost and complexity of hypervelocity impact experiments has been a limiting factor in the study of hypervelocity impact phenomenology. The aerospace community would benefit greatly from a low-cost facility capable of providing a mass-velocity analog to the MOD threat. Such a facility with *in situ* measurement capabilities enabling quantitative characterization of impact phenomena, such as debris cloud formation and evolution would strongly support the development of foundational knowledge and promote advances in spacecraft shield design.

* Corresponding author. Tel.: 1-626-395-3664
E-mail address: jmmihaly@caltech.edu

doi:10.1016/j.proeng.2013.05.041

1.1 Experimental Facility

To address the inherent challenges in understanding hypervelocity impact phenomenology, the California Institute of Technology, in a joint effort with NASA Jet Propulsion Laboratory, has established the Small Particle Hypervelocity Impact Range (SPHIR). The light-gas gun system used in this facility was designed, developed and fabricated by engineers at the Southwest Research Institute [1] and installed at Caltech in 2006. This facility [2] utilizes a two-stage light-gas gun with a 1.8 mm bore diameter launch tube capable of producing mass-dependent velocities ranging from 2 to 10 km/s. Most commonly, the facility is used to launch 5.5 mg Nylon 6/6 right cylinders (L/D = 1) to impact speeds between 5 and 7 km/s. The facility has also been used to accelerate 3.6 mg Nylon 6/6 spheres and 22.7 mg 440C steel spheres to impact speeds ranging from 5 to 6 km/s and 2 to 3 km/s, respectively. The impactors are launched, without a sabot, into a 1 m x 1 m x 2 m target chamber which is evacuated to a selectable pressure between 1 and 50 Torr.

The impactor velocity is measured using a Photron SA-1 FASTCAM high-speed camera [2]. Typically, this camera is operated at 150,000 frames per second. When the impactor is traveling at greater than 3km/s, the low-pressure atmosphere (as low as 1 Torr) in the evacuated target chamber is ionized as a sheath surrounding and trailing the impactor. This hot plasma sheath radiates sufficient light to enable high-speed imaging of the projectile location by self-illumination. Measurement of the position of the impactor ahead of the target and the time of flight to the target enables determination of the impact speed. The continuously recording, "looping" camera is triggered by the target impact flash, which is detected with a photodiode.

2. Laser Side-Lighting System

Historically, flash x-ray systems have been used [3-5] to observe and analyse the evolution of debris clouds. High-speed photography has also provided an alternative to the imaging of hypervelocity impact debris formation [6]. Advances in modern digital photography have improved both the quality and utility of high-speed photography as a method to study debris phenomena in hypervelocity impact experiments [7]. Such digital photography systems [8] typically utilize flash lamps to provide diffuse white light as an illumination source. Coherent laser light has also been recently implemented as the basis for diagnostics used in the study of ejecta [9] and debris [10] phenomena.

The Laser Side-Lighting System (LSL) described herein, which utilizes a monochromatic, collimated, and coherent light from a continuously operated laser, provides several advantages over other imaging techniques used to observe hypervelocity impact events. The use of collimated light not only enables high-speed imaging of the event with low exposure times (15 ns), but is capable of doing so with relatively low illumination intensities (600 mW).

The laser side-lighting system with an enclosed free beam provides several operational benefits *vis a vis* flash lamp and flash x-ray systems. The continuous operation of the laser illumination source produces a relatively constant illumination source throughout the entire period of the experiment, offering a solution of reduced operational complexity compared to pulsed laser photography systems [11]. Furthermore, given that the illumination source can be turned on before an experiment, this system is advantageous for facilities without a reliable method to pre-trigger the illumination source. Therefore, this laser illumination source reduces the complexity of triggering the instrumentation during the experiment.

The use of coherent light allows the LSL system, with small modification, to be used for several interferometric techniques such as schleiren imaging [12] and Coherent Gradient Sensing [13] to measure the impact phenomena. Lastly, the use of directed (collimated), monochromatic light does not interfere with any simultaneous spectroscopic measurements of the impact event during experiments.

2.1 Hardware

The Laser Side-Lighting System produces side-profile shadowgraphs using a Cordin 214-8 gated, intensified CCD camera. The Cordin camera contains 4 double-exposed CCD sensors to provide 8 images with 1000 x 1000 pixel resolution. The camera is capable of providing exposure and inter-frame times as low as 10 ns. The second exposure recorded on a given CCD must be delayed at least 3.7 μs from the first exposure to allow the corresponding micro-channel plate (MCP) intensifier to reset. However, four consecutive images may be obtained by using each of the four CCDs once. This mode enables a maximum framing rate of 50 x 10^6 fps.

A Coherent Verdi V6 diode-pumped solid-state laser is used to provide 532 nm wavelength (continuous wave) light as the illumination source. The laser beam is expanded to a 10 cm diameter collimated beam using two Keplerian beam expanders and then directed into the target tank. A mirror is used to steer the laser illumination towards an imaging solution consisting of a Keplerian beam reducer, a focusing lens, and the Cordin camera's field lenses. The Verdi V6 laser is capable of producing 6 Watts of illumination intensity. Given that a small fraction (approximately 10%) of the potential laser power is required to provide sufficient illumination intensity, a more uniform intensity can be delivered to the high-

speed camera. This is achieved through use of only the laser beam's center, which is isolated by over-expansion of the beam before collimation in the second Keplerian beam expander.

2.2 System Setup and Specifications

The laser illumination provided by the Verdi V6 laser is delivered into the target tank orthogonal to the impactor velocity vector. Figure 1 provides a conceptual illustration of the LSL system setup. The LSL system therefore provides a series of shadowgraph images which have a perspective similar to the flash x-ray technique used by Piekutowski [4]. The primary distinction of this method from flash x-ray is that the shadowgraphs generated by this method are produced by the absorption of laser illumination by debris particles and subsequent interference of the coherent light. Constructive interference of the collimated laser source is created by gradients in the index of refraction corresponding to gradients in density, pressure, and temperature of the atmosphere surrounding the debris.

The current, maximum field of view with this system is circular and defined by the diameter of the expanded laser beam, 100 mm. To utilize all of the pixels in the square 1000 x 1000 pixel CCDs of the Cordin camera, the field of view can be adjusted to a square of approximately 70 mm x 70 mm. This corresponds to an image resolution of approximately 0.07 mm/pixel. Finer resolutions and smaller fields of view with higher image resolution are also possible.

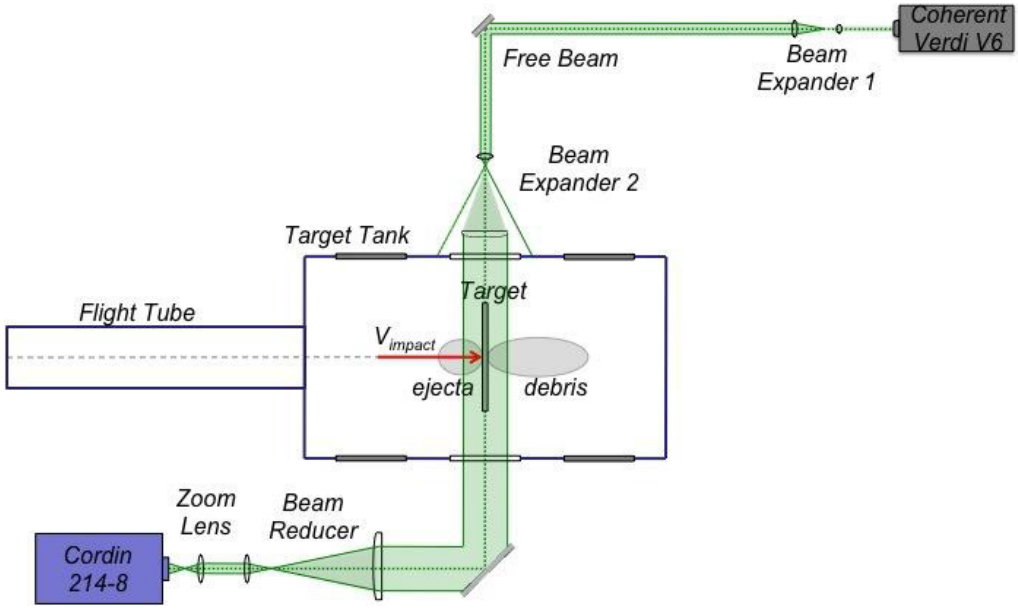

Fig. 1. The Laser Side-Lighting System (illustration not to scale).

A laser power of 600 mW is adequate to observe the hypervelocity impact event with exposure times as small as 15 ns. At the impact speeds typically produced with the SPHIR light gas gun (5 to 7 km/s), this exposure time is adequate to prevent image blur that can result from the motion of the features in the image. Furthermore, the short exposure time coupled with the collimated illumination source prevents the observed impact phenomena from being masked by camera pixel saturation from the impact flash.

As with the high-speed camera used to measure impact speed, the Cordin camera used in the LSL system is triggered by the impact flash at the target. This method is robust and consistent; however, it has an inherent limitation: there is a short delay between first contact with the target and the development of an impact flash bright enough to register on the photo diode. This creates an uncertainty in the time of initial contact between impactor and target. However, the time between the camera images is known very accurately (with an uncertainty less than 10 ns) and facilitates the accurate measurement of debris cloud evolution. Triggering of the LSL system is not limited to this triggering method and other triggering systems, such as a velocity comparator, could be used if available.

3. Image Analysis

The LSL system has been used to observe d = 1.8 mm diameter Nylon 6/6 right cylinders (L/d = 1) impacting 6061-T6 aluminum target plates at speeds between 5 and 7 km/s. A characteristic result for a h = 1.5 mm thick aluminum target impacted at 5.54 km/s is provided in Figure 2. As shown, the formation of ejecta in front of the target and debris behind the target can be observed up-range (left) and down-range (right) from the target, respectively. The ejecta up-range of the target is consistently observed to be highly asymmetric, which is believed to be a consequence of impactor geometry and impactor tumbling.

Note that the time-stamps labelling each image refer to the time from triggering. Diffraction patterns (large bullseye rings) in the background illumination are present in all of the images shown below. These artifacts are produced by internal reflections in optics inside the Cordin camera, which lack anti-reflection coatings. For the hardware currently presented, these aberrations are unavoidable, differ slightly on each CCD and typically have minimal effect on the image processing. However, in principle these aberrations can be eliminated in future LSL systems with the use of anti-reflection lenses throughout the imaging system.

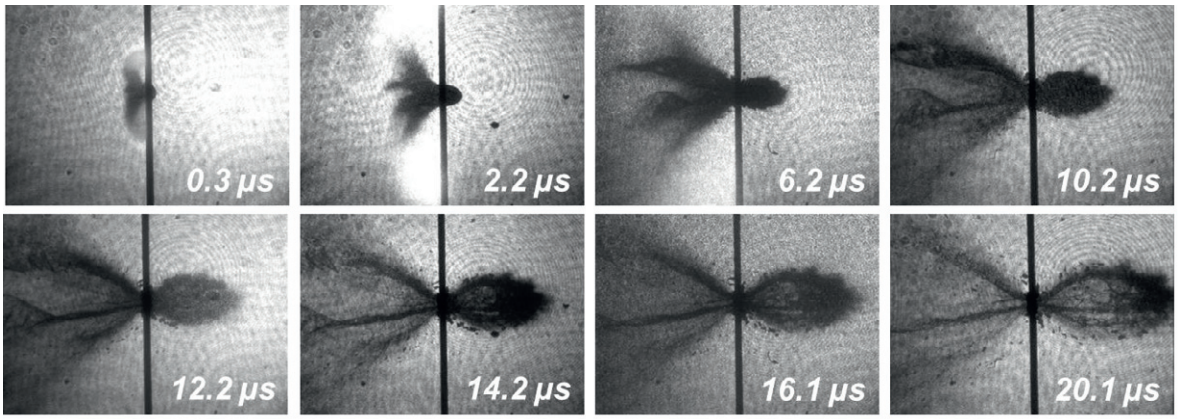

Fig.2. A h = 1.5 mm 6061-T6 aluminum target plate impacted at 5.5 km/s by a d = 1.8 mm Nylon 6/6 right cylinder at 0 degrees target obliquity. The impactor travelled from left to right and the target chamber pressure is 1.2 Torr.

3.1 Debris Cloud Measurement

An edge-finding algorithm has been developed to identify the boundary of the debris front in each image of the earlier images. The algorithm analyzes grayscale data from each image along lines in the longitudinal z-direction (constant y). Along each line, grayscale values are considered as a moving average. The moving standard deviation and gradient of this moving average of grayscale is then computed. The boundary is then identified at points where the gradient is large and positive and the standard deviation is a maximum. Note that in the convention used here, a white pixel has a grayscale of 255. Figure 3 provides an example of this algorithm and edge-finding result with an illustration of the defined boundary and corresponding grayscale analysis.

The uncertainty of the debris-front position can then be quantified based on the length of the transition region of grayscale and standard deviation. In the example shown in Figure 3, this would correspond to an error of approximately 5 pixels or less resulting in an accuracy of ± 0.3 mm. This methodology provides a consistent way to define debris-front position in a single image. The method is applied to each image in the sequence of images obtained during an experiment. An example result is shown in Figure 4, which illustrates a measured debris front in one image while plotting the positions of debris fronts taken from the following two images (taken 0.9 and 1.9 micro-seconds later). This data can be used to measure the longitudinal speed of the debris produced as a function of radial distance from the impact site. Measurement of the speed of debris thrown from the target early in the formation of the debris cloud provides one metric for comparison and validation of numerical simulations [14]. Furthermore, this method provides a regular methodology to quantify asymmetrical debris front velocities in each experiment. Given the described accuracy of the debris position measurement and excellent temporal uncertainty of the Cordin camera (less than 10 nanoseconds), measurement of the debris velocity is computed with an accuracy of ± 0.1 km/s. In the example presented in Figure 4, a 6.3 km/s impact of a 1.8 mm Nylon right-cylinder (L/D=1) on a 1.5 mm thick 6061-T6 aluminum plate produces an initial debris front velocity (separate but collinear with the impactor velocity vector) of 1.8 km/s.

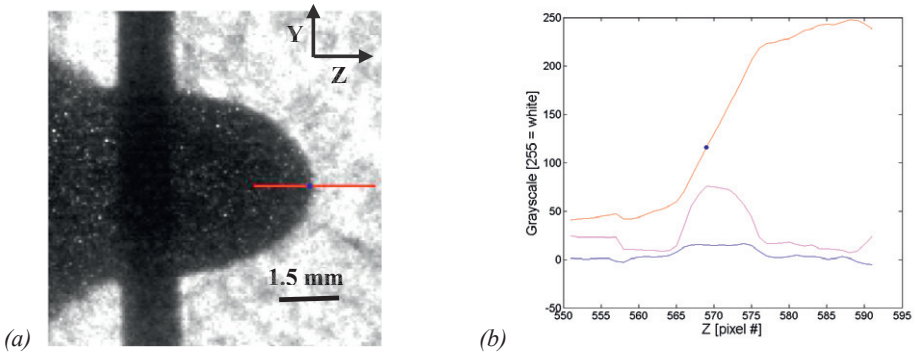

Fig. 3. (a) Enlarged view of the image from Figure 2. The blue dot is the boundary identified by the described edge-finding algorithm. Grayscale values along the red-line are analyzed in the adjacent image. (b) The moving average of the grayscale is plotted in red. The pink line is the moving standard deviation of the grayscale and the blue line is the gradient of the grayscale.

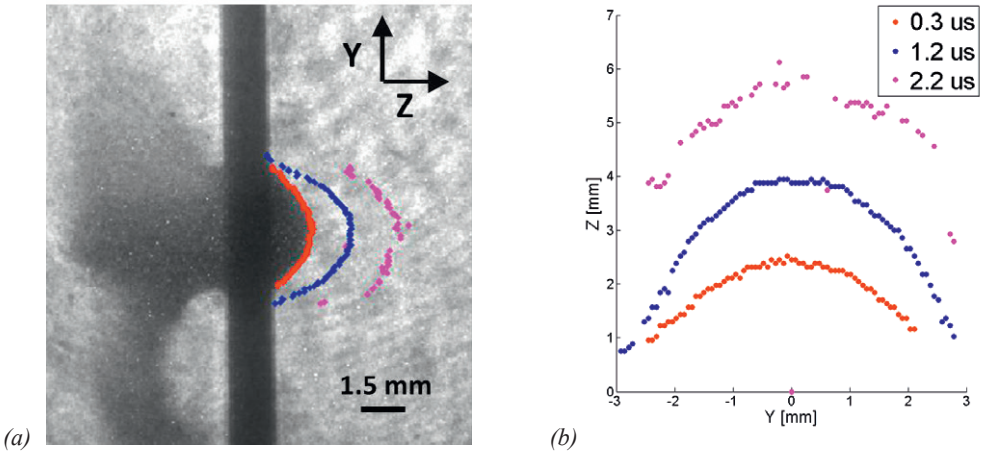

Fig. 4. (a) The debris-front is identified (in red) for the image shown using the described edge-finding algorithm. The debris-fronts identified in the subsequent images (0.9 and 1.9 micro-seconds later) are painted in blue and magenta. (b) The positions of the identified debris fronts are plotted with respect to the impact location.

3.2 High-Pressure Measurements

The use of collimated, coherent light in the LSL system significantly increases the observable impact features in experiments where the atmospheric pressure in the target chamber is increased above the nominal 1 Torr. At higher pressures, waves emanating from the impact site are visible much like they are in schleiren shadowgraphs [12]. The observation of these phenomena is enabled by strong gradients in the index of refraction of the rarefied atmosphere constructively interfering with the coherent light source. An example of this observation is provided in Figure 5 for a h = 0.5 mm plate impacted at 4.7 km/s in 50 Torr atmospheric pressure. Slight defocussing of the imaging system enables improved contrast of the observed shock as a result of caustic effects. Measurement of these waves can enhance understanding of the temporal sequence of the impact phenomena.

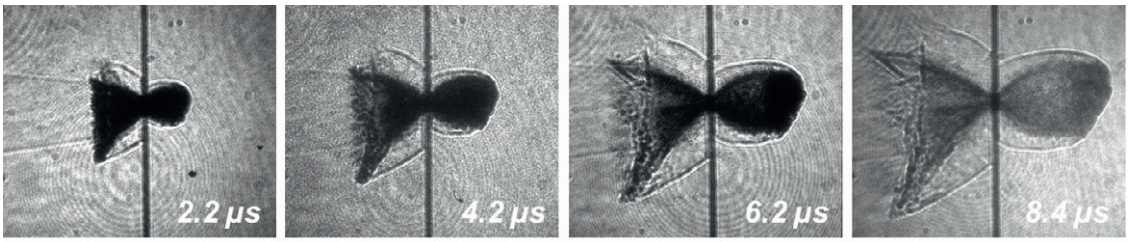

Fig.5. A h = 0.5 mm 6061-T6 aluminum target plate impacted at 4.7 km/s by a d = 1.8 mm Nylon 6/6 right cylinder at 0 degrees target obliquity. The impactor travelled from left to right and the target chamber pressure is 50 Torr.

3.3 Future Work

The LSL technique is currently being utilized in an extended series of experiments to characterize debris cloud and ejecta behaviour and other impact phenomena produced by d = 1.8 mm Nylon 6/6 right cylinders impacting 6061-T6 aluminum plates at impact speeds between 5 and 7 km/s. The campaign features significant replication of experiments with identical test conditions in order to characterize the variation inherent in the impact phenomena. Aluminum target plate thicknesses have been selected to provide a variety of plate deformation and perforation mechanisms. Previous work [15] at the SPHIR facility involved uncertainty quantification and validation of numerical models simulating high-speed impact. Measurements obtained using the LSL system for Nylon cylinders impacting aluminum plates will be implemented in a similar campaign comparing results to those of a numerical simulation [14]. Additionally, LSL results will be complemented by a suite of *in situ* and *post mortem* optical diagnostics. Such diagnostics will relate results to the *post mortem* damage of the target and help describe the content, scale and lethality of the debris cloud.

Acknowledgements

This material is based upon work supported by the Department of Energy National Nuclear Security Administration under Award Number DE-FC52-08NA28613. The authors would also like to thank Mike Mello for his assistance with the optomechanical design of the LSL system and Petros Arakelian for his assistance in installing the optical benches and safety features.

References

[1] Grosch, D. J., Riegel, J.P., 1993. Development and Optimization of a "Micro" Two-Stage Light-Gas Gun, International Journal of Impact Engineering 14, p. 315.
[2] Mihaly, J.M., Lamberson, L.E., Adams, M.A., Rosakis, A.J., 2010. "A low cost, small bore light-gas gun facility," Proceedings of the 11th Hypervelocity Impact Symposium, p. 675-686.
[3] Friend, W.H., Murphy, C.L, Gough, P.S., Review of meteoroid-bumper interaction studies at McGill University. NASA CR-54858
[4] Piekutowski, A.J., Characteristics of Debris Clouds Produced by Hypervelocity Impact of Aluminum Spheres with Thin Aluminum Plates, International Journal of Impact Engineering 14, p. 573
[5] Piekutowski, A.J., 1987. Debris Clouds Generated by Hypervelocity Impact of Cylindrical Projectiles with Thin Aluminum Plates, International Journal of Impact Engineering 5, p. 509
[6] Kassel, P.C., DiBattista, J.D., 1971. An ultra-high-speed photographic system for investigating hypervelocity impact phenomena. NASA TN D-6128
[7] Francesconi, A., Pavarin, D., Giacomuzzo, C., Angrilli, F., 2006. Impact experiments on low-temperature bumpers, International Journal of Impact Engineering 33, p. 264 – 272.
[8] Putzar, R., Schaefer, F., Lambert, M., Vulnerability of spacecraft harnesses to hypervelocity impacts, International Journal of Impact Engineering 35, p. 1728 – 1734.
[9] Hermalyn, H., Schultz, P. H., Heineck, J.T., 2009. "Early Stage Ejecta Velocity Distribution," 40th Lunar and Planetary Science Conference.
[10] Zhang, Q., Chen, Y., Huang, F., Long, R., 2008. Experimental Study on Expansion Characteristics of Debris Clouds Produced by Oblique Hypervelocity Impact of LY12 Aluminum Projectiles with thin LY12 aluminum plates, International Journal of Impact Engineering 35, p. 1884
[11] Isbell, W.M., 1987. Historical overview of hypervelocity impact diagnostic technology. International Journal of Impact Engineering 5, p. 389 – 410.
[12] Settles, G. S., 2001. *Schlieren and shadowgraph techniques: Visualizing phenomena in transparent media,* Berlin:Springer-Verlag.
[13] Rosakis, A.J.,1993. Two Optical Techniques Sensitive to Gradients of Optical Path Difference: The Method of Caustics and the Coherent Gradient Sensor (CGS) in *"Experimental Techniques in Fracture*" J. Epstein Editor, p. 327
[14] Li, B., Perotti, L., Adams, M., Mihaly, J. M., Rosakis, A.J., Stalzer, M., Ortiz, M. , 2012. "Large scale Optimal Transportation Meshfree (OTM) simulations of hypervelocity impact" 12th Hypervelocity Impact Symposium.
[15] M. Adams, A. Lashgari, B. Li, M. McKerns, J. Mihaly, M. Ortiz, H. Owhadi, A.J. Rosakis, M. Stalzer, T.J. Sullivan, Rigorous model-based uncertainty quantification with application to terminal ballistics - Part II. Systems with uncontrollable inputs and large scatter, Journal of the Mechanics and Physics of Solids, ISSN 0022-5096